POSSIBILITY OF LONGITUDINAL BUNCH COMPRESSION IN PETRA III

I. Agapov *, European XFEL GmbH, Hamburg, Germany,
S. Tomin , NRC Kurchatov Institute, Moscow, Russia,
and European XFEL GmbH, Hamburg, Germany
R. Wanzenberg, DESY, Hamburg, Germany

Abstract

A scheme of short bunch production in storage rings using a longitudinally focusing insertion was presented in [1]. In this work we study the possibility of integrating such insertion into the PetraIII storage ring. In particular, we discuss possible optics solutions to integrate RF stations, chicane-type delay sections, and the undulators into existing ring geometry.

INTRODUCTION

A possibility of short bunch production in storage rings using compression followed by decompression was presented in [1]. There it was also shown that the scheme can be used to operate a high gain FEL in a low emittance storage ring such as Petra III [2]. At Petra III several straight sections are presently available, e.g. one of about 70 m length in the North-West (NW) section (see Fig. 1) The scheme is briefly introduced in first section. Possible solutions in terms of electron optics are discussed in the second section. As part of the compression and decompression, sections with variable R_{56} of opposite signs are required. While a slight modification of an arc provides a section with necessary positive R_{56}, the negative R_{56} requires larger modification to the optics. It turns out that designing such a section is rather challenging due to issues with emittance preservations. A short chicane with rather strong bending magnets could increase the equilibrium emittance significantly and installation of such a chicane for large negative R_{56} does not seem feasible. However, a modification to the scheme where both chicanes have positive R_{56} requires very minor changes to the present machine layout (apart from installing two RF sections) at the cost of slightly more complex longitudinal dynamics.

SCHEME

The scheme proposed in [1] is based on the observation that longitudinal focusing similar to the bunch compression in linac-based FELs could potentially be run in a storage ring. An RF section followed by a section with energy-dependent time delay acts as a 'compressor', and the mirror reflection of this setup acts as a 'decompressor'. The scheme is sketched in Fig. 2. With the peak bunch current thus increased by an order of magnitude and small emittance of a ring such as Petra III operation of a high gain ring FEL could be potentially possible for soft x-rays of energies below approx. 1-2 keV. The longitudinal phase space map for the insertion is

$$M = M_{RF2} \cdot M_{C2} \cdot M_{C1} \cdot M_{RF1} \tag{1}$$

where the magnetic section maps are given by matrices

$$M_{C1,C2} = \begin{pmatrix} 1 & R_{56}^{(1,2)} \\ 0 & 1 \end{pmatrix} \tag{2}$$

and the RF section maps are

$$M_{RF1,RF2} : \begin{pmatrix} t \\ p \end{pmatrix} \rightarrow \begin{pmatrix} t \\ p + V^{(1,2)} \sin(\omega_{RF} \cdot t) \end{pmatrix} \tag{3}$$

Here t and p are longitudinal coordinates usually measured in meters and relative energy units, R_{56} is the standard notation for dispersive time delay, $V^{(1,2)}$ are total RF voltages for the compressor and the decompressor, and ω_{RF}

Table 1: PETRA III beam parameters [2]

Parameter	High charge	Low charge
Beam energy	6 GeV	
Circumference	2304 m	
No. bunches	40	960
Emittance ε_x	$1.2 \cdot 10^{-9}$ m · rad	
Emittance ε_y	$1.2 \cdot 10^{-11}$ m · rad	
Energy spread	10^{-3} (6 MeV)	
Bunch charge	19 nC	0.8 nC
Bunch length	44 ps (rms)	
Peak current	170 A	7 A
Average current	100 mA	100 mA
Long. damping time	8 msec	
Transv. damping time	16 msec	

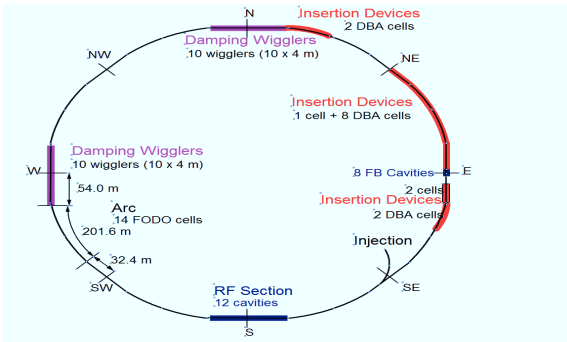

Figure 1: Present layout of Petra III

* ilya.agapov@xfel.eu

ISBN 978-3-95450-168-7

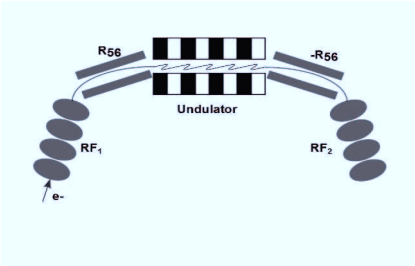

Figure 2: Concept

the RF angular frequency. One can easily check that by choosing $R_{56}^{(1)} = -R_{56}^{(2)}$ and $V^{(1)} = -V^{(2)}$ the combined transfer map reduces to a unit matrix. We will refer to this as the positive-negative R_{56} option. One can also choose the decompressor option with $R_{56}^{(1)} = R_{56}^{(2)}$ and $V^{(1)} = V^{(2)}$. The whole insertion map is not unity but in linear approximation and for diminishing energy spread it is a phase space rotation by 180^0 which maps the distribution onto itself. We will refer to this as the positive-positive R_{56} option. While the positive-negative map is unity and can be applied arbitrarily many times without distorting the phase space, this is not the case for the positive-positive map. When the bunch length and the RF frequency are such that the bunch is well within the RF bucket, the distortion is relatively week. Fig. 3 shows the effect of the map for 44 ps rms bunch and 1.3 GHz RF for 1000 turns, which is the longitudinal damping time at Petra III. Storing the beam in this situation should be possible. With longer bunches or higher RF frequencies the effect of the map is getting more nonlinear, many particles are lost to instability and the phase space becomes more complicated (see Fig. 4). In this situation the beam is not stored properly. It would be interesting to study the shape of equilibrium beam distribution when the radiative damping is taken into acount.

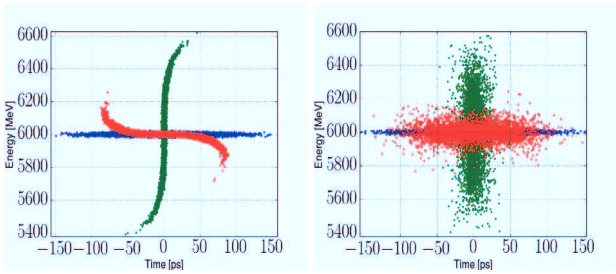

Figure 3: Effect of a map with both R_{56} positive, 1.3 GHz. Initial longitudinal phase space distribution is shown in blue, the compressed and the decompressed distributions are shown in green and red. Left: effect of one turn. Right: effect of 1000 turns.

Another possible fundamental limitation is the energy spread growth due to the FEL process. FEL simulations suggest that for the 1 keV radiation wavelength and the peak output power below about 1 GW, the FEL-induced energy spread is dominated by the energy spread from spontaneous

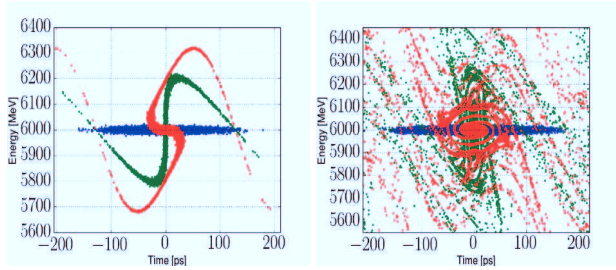

Figure 4: Effect of a map with both R_{56} positive, 3.9 GHz. Initial longitudinal phase space distribution is shown in blue, the compressed and the decompressed distributions are shown in green and red. Left: effect of one turn. Right: effect of 1000 turns.

radiation (see Fig. 5). Moreover, this energy spread is induced when the beam is compressed and thus has a large energy spread (about 1-2%), so that the induced energy spread is further reduced by the compression factor after decompression.

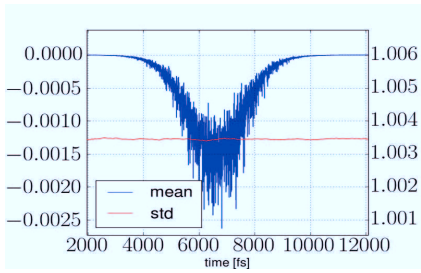

Figure 5: Mean relative energy loss (blue, left axis) and rms relative energy spread (red, right axis) in units of 10^{-3} inside the electron bunch after the undulator for 20x compression, with approx. 50MW peak power. The energy spread includes the initial energy spread of 10^{-3}.

OPTICS

To achieve the compression factor of 20, a possible option is to have a 17 m long 1.3 GHz RF section and R_{56} = 40 cm for compressor (-40 cm for decompressor). Here we consider the optics design for this value. If $\xi_x(s)$ is the dispersion created along a section and ρ is the bending angle then $R_{56} \propto \int \xi_x(s)/\rho(s)ds$. Positive R_{56} is achieved by creating large dispersion in bends (and then closing it with focusing if necessary). Negative R_{56} is achieved by either creating large dispersion and then putting the beam through bends of opposite sign, or by creating negative dispersion in bends, or by both. In this respect, the limitation is only the available length and the maximum achievable magnetic field in the bends. It turns out that a more severe additional requirement on the optics is that the contribution to the equilibrium emittance is small. The equilibrium emittance (plane x only) is given by

$$\epsilon_x = C_q \gamma^2 \frac{\mathcal{I}_5}{\mathcal{I}_2 - \mathcal{I}_4} \quad (4)$$

ISBN 978-3-95450-168-7

$$\mathcal{I}_5 = \left\langle \frac{\mathcal{H}}{|\rho|^3} \right\rangle \quad \mathcal{H} = \beta_x \eta_x'^2 + 2\alpha_x \eta_x \eta_x' + \gamma_x \eta_x^2 \qquad (5)$$

$$\mathcal{I}_2 = \left\langle \frac{1}{\rho^2} \right\rangle \quad \mathcal{I}_4 = \left\langle \frac{\eta_x}{\rho^3}\left(1 + 2\rho^2 k\right) + 2\frac{\eta_x k}{\rho} \right\rangle \qquad (6)$$

where $C_q = 3.83 \times 10^{-13}$ m. The dependence of emittance on the third power of the bending angle via $\mathcal{I}_5$ makes it difficult to achieve low emittances with strong bending. On the other hand creating sufficiently large negative R_{56} requires large dispersion and/or large bending angles. The arc upstream from the NW straight section has R_{56} about 40 cm. To close the dispersion in the arcs the last dipole is moved one position ahead (so-called 'missing dipole scheme'). The compressor layout would require putting RF stations at the end of straigh section West, and midifying the arc to match the optics to the undulator section in the NW straight section. The latter can be achieved by moving the last dipole one position back to free aditional space and providing individual power supplies to 6 last quadrupoles in the arc. The resulting optics functions are shown in Fig. 6. This modification does not affect the equilibrium emittance noticably. The undulator is assumed to 2 cm period, with undulator K parameter in the range of 4 - 9, consisting of 2 m long sections with $\langle\beta\rangle = 5$ m FODO optics and taking up the whole straight section.

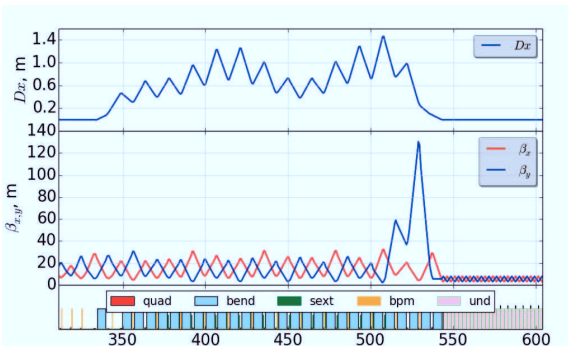

Figure 6: Upstream arc and undulator section optics. In the undulator section $\langle\beta_X\rangle = \langle\beta_Y\rangle = 5$ m. All optics calculations in the paper are done with OCELOT [3].

Negative R_{56} is hard to achieve with minimal modifications to the downstream arc. It is possible to replace first few tens of meters of the arc with a chicane-type line and increase the bending angle in the rest of the arc. However the equilibrium emittance is sensitive to adding strong bending magnets, and the chicane parameters have to be selected carefully. Following [4] one can estimate the theoretical minumum on the contribution to radiation integrals for single magnets. For Petra III the equilibrium emittance is mostly determined by the value of $\mathcal{I}_5$ which is equal to $6.6 \cdot 10^{-6}$ m^{-1} without taking damping wigglers into account. The equlibrium emittance is then 5 nm rad. With damping wigglers the emittance is 1.2 nm rad. For a 5 m long magnet with bending angle 0.05 rad and the beta function in the range of 10-30 m the theoretical minimum to $\mathcal{I}_5$ is about $2 \cdot 10^{-7}$ m^{-1}, whereas for same magnet with bending angle of 0.1 rad it is already $2 \cdot 10^{-6}$ m^{-1}. Using magnets of latter type for the chicane without increasing the emittance significantly is not possible. On the other hand, using weak magnets will result in long chicane length. This would have to be compensated by much stronger bending in the rest of the arc. The setup will also not fit into existing tunnel. An example of optics matched for low $\mathcal{I}_5$ contribution (30 % of existing value) is shown in Fig. 7. This line requires 80 m and can only achieve R_{56} = - 10 cm. On the other hand, the downstream arc optics for the positive-positive option is just a mirror reflection of the optics shown in Fig. 6, and is achieved with minimal rematching of the undulator section to the arc. The equilibrium emittance is the same as in the existing machine. In all this considerations we neglected the influence of the insertion devices, which will further reduce the equilibrium emittance depending on the undulator K parameter.

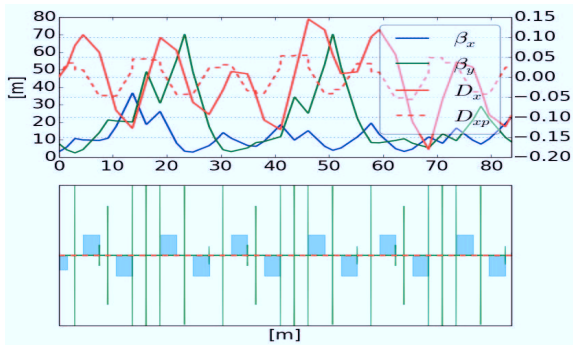

Figure 7: Bunch decompressor optics, for $R_{56} = -10$ cm and $\mathcal{I}_5 = 2 \cdot 10^{-6}$ m^{-1}

CONCLUSION

We showed that the integration of the longitudinal focusing insertion with two 'chicane' sections of opposite R_{56} is demanding in terms of space. On the other hand, the longitudinal focusing with two 'chicane' sections of same R_{56} can be achieved by minor modifications to the existing layout. The second option exhibits more complex dynamics in the longitudinal phase space but long-term beam stability is anticipated. The equilibrium beam dimensions under radiative excitation and damping and the problem of halo formation are to be studied further.

ACKNOWLEDGEMENTS

The authors wish to thank S. Molodtsov, G. Geloni, and R. Brinkmann. S. Tomin acknowledges partial support from BMBF grant EDYN EMRAD.

REFERENCES

[1] I. Agapov and G. Geloni, "Storage ring XFEL with longitudinal focusing", in Proceedings of FEL 2014, Basel, Switzerland (2014); I. Agapov, arXiv:1311.7428 [physics.acc-ph]

[2] K. Balewski et al. (eds.), “Petra III : A Low Emittance Synchrotron Radiation Source", Technical Design Report, DESY (2004)

[3] I. Agapov et al., “OCELOT: a software framework for synchrotron light source and FEL studies", Nucl. Instr. Meth. A. 768 (2014) pp. 151-156

[4] C. Wang, “Minimum emittance in storage rings with uniform or nonuniform dipoles.", Phys. Rev. ST Accel. Beams 12, 061001 (2009)

ISBN 978-3-95450-168-7